

RESEARCH

Open Access



# Extracellular vesicle-microRNAs mediated response of bovine ovaries to seasonal environmental changes

Ahmed Gad<sup>1,2</sup>, Kamryn Joyce<sup>3</sup>, Nico Graham Menjivar<sup>1</sup>, Daniella Heredia<sup>3</sup>, Camila Santos Rojas<sup>3</sup>, Dawit Tesfaye<sup>1\*</sup> and Angela Gonella-Diaza<sup>3</sup>

## Abstract

**Background** Among the various seasonal environmental changes, elevated ambient temperature during the summer season is a main cause of stress in dairy and beef cows, leading to impaired reproductive function and fertility. Follicular fluid extracellular vesicles (FF-EVs) play an important role in intrafollicular cellular communication by, in part, mediating the deleterious effects of heat stress (HS). Here we aimed to investigate the changes in FF-EV miRNA cargoes in beef cows in response to seasonal changes: summer (SUM) compared to the winter (WIN) season using high throughput sequencing of FF-EV-coupled miRNAs. In addition to their biological relevance, the potential mechanisms involved in the packaging and release of those miRNAs as a response to environmental HS were elucidated.

**Results** Sequencing analysis revealed that an average of 6.6% of the EV-RNA mapped reads were annotated to bovine miRNAs. Interestingly, miR-148a, miR-99a-5p, miR-10b, and miR-143 were the top four miRNAs in both groups accounting for approximately 52 and 62% of the total miRNA sequence reads in the SUM and WIN groups, respectively. A group of 16 miRNAs was up-regulated and 8 miRNAs were down-regulated in the SUM compared to the WIN group. Five DE-miRNAs (miR-10a, miR-10b, miR-26a, let-7f, and miR-1246) were among the top 20 expressed miRNA lists. Sequence motif analysis revealed the appearance of two specific motifs in 13 out of the 16 upregulated miRNAs under HS conditions. Both motifs were found to be potentially bonded by specific RNA binding proteins including Y-box binding proteins (YBX1 and YBX2) and RBM42.

**Conclusion** Our findings indicate that FF EV-coupled miRNA profile varies under seasonal changes. These miRNAs could be a good indicator of the cellular mechanism in mediating HS response and the potential interplay between miRNA motifs and RNA binding proteins can be one of the mechanisms governing the packaging and release of miRNAs via EVs to facilitate cellular survival.

**Keywords** Follicular fluid, Extracellular vesicles, miRNA, Heat stress, Beef cows

\*Correspondence:

Dawit Tesfaye

dawit.tesfaye@colostate.edu

Full list of author information is available at the end of the article



This is a U.S. Government work and not under copyright protection in the US; foreign copyright protection may apply 2023. **Open Access** This article is licensed under a Creative Commons Attribution 4.0 International License, which permits use, sharing, adaptation, distribution and reproduction in any medium or format, as long as you give appropriate credit to the original author(s) and the source, provide a link to the Creative Commons licence, and indicate if changes were made. The images or other third party material in this article are included in the article's Creative Commons licence, unless indicated otherwise in a credit line to the material. If material is not included in the article's Creative Commons licence and your intended use is not permitted by statutory regulation or exceeds the permitted use, you will need to obtain permission directly from the copyright holder. To view a copy of this licence, visit <http://creativecommons.org/licenses/by/4.0/>. The Creative Commons Public Domain Dedication waiver (<http://creativecommons.org/publicdomain/zero/1.0/>) applies to the data made available in this article, unless otherwise stated in a credit line to the data.

## Background

Global climate change directly impacts the livestock sector due to continued increases in atmospheric temperatures and as a result, animals are exposed to more adverse conditions of heat stress (HS). The global economic losses amid the dairy and beef industry due to HS are estimated to be between \$14.89 – 39.94 billion per year by the end of the century [1]. This primarily stems from the significant impact of HS on animal productivity and the continued decline in fertility and reproductive performance [2]. The harmful effects of HS on ovarian functions and subsequent oocyte developmental competence are one of the main reasons driving reduced fertility [3]. The development of novel alternative strategies to mitigate the negative impacts of HS on reproductive function requires a more comprehensive understanding of heat-induced molecular alterations at the cellular level.

In bovine, follicular development is a lengthy process starting from the growth of primordial follicles to the preovulatory stage. Effects of maternal hyperthermia during specific stages of follicular growth and development may significantly affect follicular growth [4], in which the carryover effects of HS have the capacity to linger for months into the cool season resulting in long-term impacts on the reproductive performance of animals [5].

Seasonal effects on cows' reproduction include different factors (e.g., feeding, daylight hours, etc.), however, the most important factor is the consequence of increased temperature and humidity that result in inadequate regulation of the cow's body temperature, a reduction in appetite and dry matter intake, reduction in duration and intensity of estrus, as well as disruption in hormonal levels [6, 7]. Several seasonal studies have reported the sensitivity of the ovarian pool of oocytes to elevated temperatures expressed as reduced developmental competence [8, 9]. Seasonal HS is known to alter steroid production and the biochemical composition of the follicular fluid (FF). For instance, FF obtained from large follicles of cows during the hot season is evidenced by lowered steroid concentrations, reduced granulosa cell (GC) viability, and impaired aromatase activity [10]. Moreover, the biochemical changes in the FF of the dominant follicle from high-producing cows exposed to HS post-partum have been evidenced by reduced concentrations of glucose, IGF-1, and cholesterol [11]. At the cellular level, cells activate heat shock proteins (HSPs) and oxidative stress response machinery as a defensive mechanism in response to HS that could ultimately lead to cell apoptosis [12]. Activated HSPs, as well as RNA transcripts, could be released by stressed cells and uptaken by other recipient cells to modulate their immunological responses against stress [13–15]. In the intrafollicular

microenvironment, such cellular communication is facilitated by the FF containing various paracrine factors important for cell–cell communication during follicular growth [16].

In the follicular microenvironment, one of the more recently discovered mechanisms that facilitate and modulate communicative measures between various cells and the oocyte is extracellular vesicles (EVs). EVs are nano-sized, membrane-bound, and evolutionarily conserved structures secreted from almost all cell types into the surrounding extracellular space and are preferentially found among almost all body fluids [17]. EVs are broadly categorized as exosomes, microvesicles, and apoptotic bodies according to their size and mode of biogenesis [18]. Their capacity to modulate intercellular crosstalk is largely through their ability to transfer various bioactive molecules, including mRNA, miRNAs, and proteins, between neighboring cells following secretion into body fluids [19]. We have recently shown that bovine GCs subjected to in vitro thermal stress release EVs harnessed with protective molecular signals that induce tolerance to recurrent thermal stress in naïve recipient cells [20]. In addition, those EVs were found to contain different miRNA profiles in response to HS. The emerging regulatory role of miRNAs in mediating the stress response in different species [21–24] sheds light on their use as potential biomarkers and/or tools to modulate the cellular stress response. Therefore, understanding the follicular responses, in terms of EV-coupled miRNAs, to HS in cows during the summer seasons will aid in determining the specific role of these miRNAs in mediating the HS response amid intrafollicular cellular communication. Here we aimed to investigate the follicular level response of beef cows to seasonal changes with regard to the FF-EV miRNA profiles. Moreover, miRNA motifs and the corresponding RNA binding proteins were identified and their potential involvement in the packaging and release of miRNAs into EVs as it relevantly correlates to cellular survival under HS conditions is elucidated.

## Materials and methods

### Animals and sample collection

The experiment was conducted at the UF/IFAS North Florida Research and Education Center (Marianna, Florida, USA). Eleven *Bos taurus* crossbreed open cows were included in the experiment after clinical and gynecological examinations. Transrectal ultrasound was conducted to evaluate ovaries and it was determined that all cows were cycling (bearing at least one CL or preovulatory follicle in one of the ovaries) and without any ovarian abnormalities (cysts, tumors, etc.) before each OPU session. The cows remain open, maintained in outdoor pens with bahia grass and fed bermudagrass hay to meet the

nutritional requirements of mature cows. Also, cows had ad libitum access to water and mineralized salt during the whole study (from winter until summer). Body weight and Body condition score (scored from 1 (thin) to 9 (fat)) were not different between winter and summer (Winter:  $580.2 \pm 20.5$  kg and BCS of  $5.0 \pm 0.0$ ; Summer:  $571.1 \pm 18.1$  kg and BCS of  $5.0 \pm 0.0$ ;  $P > 0.05$ ). Ovum pick-up (OPU) sessions were conducted by a single operator in two different seasons: Winter (January 2021) and Summer (August 2021). Before each OPU session cows were stimulated to increase the number of follicles. Briefly, on a random day of the estrus cycle (Day 0) a progesterone device (Eazi-Breed CIDR Cattle Insert; Pfizer Animal Health, New York, NY, USA) was inserted in the vagina and a single dose of a GnRH analog (Factrel, 2 mL, im, Pfizer Animal Health) was administered. Follicular growth stimulation was conducted by giving 3 injections of FSH (Folltropin V, im, Vetoquinol, Bertinoro, Italy). On day 3, 3 ml (equivalent to 105 IU) of FSH were administered in the morning and afternoon. On day 4, 2 ml of FSH were administered in the morning (equivalent to 70 IU). Finally, on day 5, the CIDR was removed and OPU was conducted in the morning. Ultrasound examinations (Esaote ultrasound, MyLabDelta Vet, with 10–5 MHz transducer) were conducted to evaluate the presence of a corpus luteum and the number of follicles at days 0 and 5.

OPU was performed using a real-time B-mode ultrasound scanner (Mindray 2200; Mindray Bio-Medical Electronics, Shenzhen, China) equipped with a 5-MHz micro-convex transducer (Mindray model 65C15EAV, Mindray Bio-Medical Electronics, Shenzhen, China) and coupled to a follicular aspiration guide (WTA, São Paulo, Brazil) and a stainless-steel guide. The follicular puncture was performed using a disposable 18 G hypodermic needle connected to a 50-mL conical tube via a suitable silicon tubing system (WTA). The pressure for aspiration was maintained using a vacuum pump (WTA model BV-003, WTA) with negative pressure adjusted between 60 and 80 mmHg. After the OPU of both ovaries, the aspiration system was replaced with a new one before conducting OPU for the next cow. The complete experimental design is presented in Fig. 1.

#### Summer vs. winter environmental conditions

As previously stated, OPU was conducted on the same animals in two different seasons. Environmental data (average minimum and maximum temperature and relative humidity) from the 3 weeks before each OPU session was collected using the Florida Automated Weather Network (FAWN; <https://fawn.ifas.ufl.edu/data/reports/>). For the winter OPU, data were collected from February 2 to 23 of 2021, and for the summer OPU, data

were collected from July 23 to August 13 of 2021. Next, the temperature humidity index (THI) was calculated using the following equation:  $THI = (1.8 \times T + 32) - [(0.55 - 0.0055 \times RH) \times (1.8 \times T - 26)]$ , where  $T$  = air temperature ( $^{\circ}C$ ) and  $RH$  = relative humidity (%) [25]. As expected, average temperature (summer:  $27.48$   $^{\circ}C$ ; winter:  $11.46$   $^{\circ}C$ ), minimum temperature (summer:  $23.14$   $^{\circ}C$ ; winter:  $6.45$   $^{\circ}C$ ), maximum temperature (summer:  $33.66$   $^{\circ}C$ ; winter:  $16.14$   $^{\circ}C$ ), and relative humidity (summer: 82%; winter: 83%) were contrasting in the summer compared with the winter. Also, when estimating the THI, the average THI in the summer was 79 while in the winter was 53. In *Bos taurus* beef cattle, a THI equivalent to 75 is an indicator of heat stress [26, 27]. Three weeks before the summer OPU session THI was always over 75, ranging from 75.47 to 82.45.

#### Isolation of extracellular vesicles from follicular fluid

Four different FF samples (pool of two animals in each) from each group were used for EV isolation. Follicular fluid samples were subjected to a series of centrifugations starting at 500  $\times g$  for 10 min to remove cells, followed by 3000  $\times g$  for 10 min to remove the cellular debris, and at 12,000  $\times g$  for 30 min to remove protein aggregates and large particles. All centrifugation steps were performed at  $4$   $^{\circ}C$ . The supernatant of FF samples was filtered through a  $0.22$   $\mu m$  sterile filter to remove particles larger than 200 nm. For the EV isolation, 2 ml of pre-centrifuged follicular samples were subjected to an ultracentrifugation procedure at 120,000  $\times g$  for 70 min at  $4$   $^{\circ}C$  using the Beckman SWTi55 rotor. The EVs pellet was washed with sterile PBS and then centrifuged again at 120,000  $\times g$  for 70 min. Finally, EVs were resuspended in 500  $\mu L$  of PBS and stored at  $-80$   $^{\circ}C$  until further characterization and analysis.

#### Morphological and molecular characterization of EVs

The presence of EV-specific proteins (CD63, TSG101, FLOT1) in the isolated EVs and the absence of a cell-specific marker protein, cytochrome C (CYCS), were verified by the immunoblotting technique as we previously described [20]. Briefly, 100  $\mu L$  of isolated EVs were lysed in 50  $\mu L$   $1 \times$  RIPA buffer and the protein extract samples were centrifuged at 12,000  $\times g$  for 30 min at  $4$   $^{\circ}C$ . Following this, protein lysates were separated in 10–12% gradient SDS-PAGE gel (Bio-Rad Laboratories, USA) at 90 V for 15 min and 125 V for 60 min and transferred onto a nitrocellulose membrane (Bio-Rad Laboratories, USA) for 1 h at 100 V. Membranes were blocked in 5% non-fat dry milk dissolved in TBST for 1 h on a shaker at room temperature. Following blocking, membranes were incubated with anti-CD63 rabbit polyclonal (1:250 System Biosciences, USA), Anti-TSG101 rabbit polyclonal (1:250

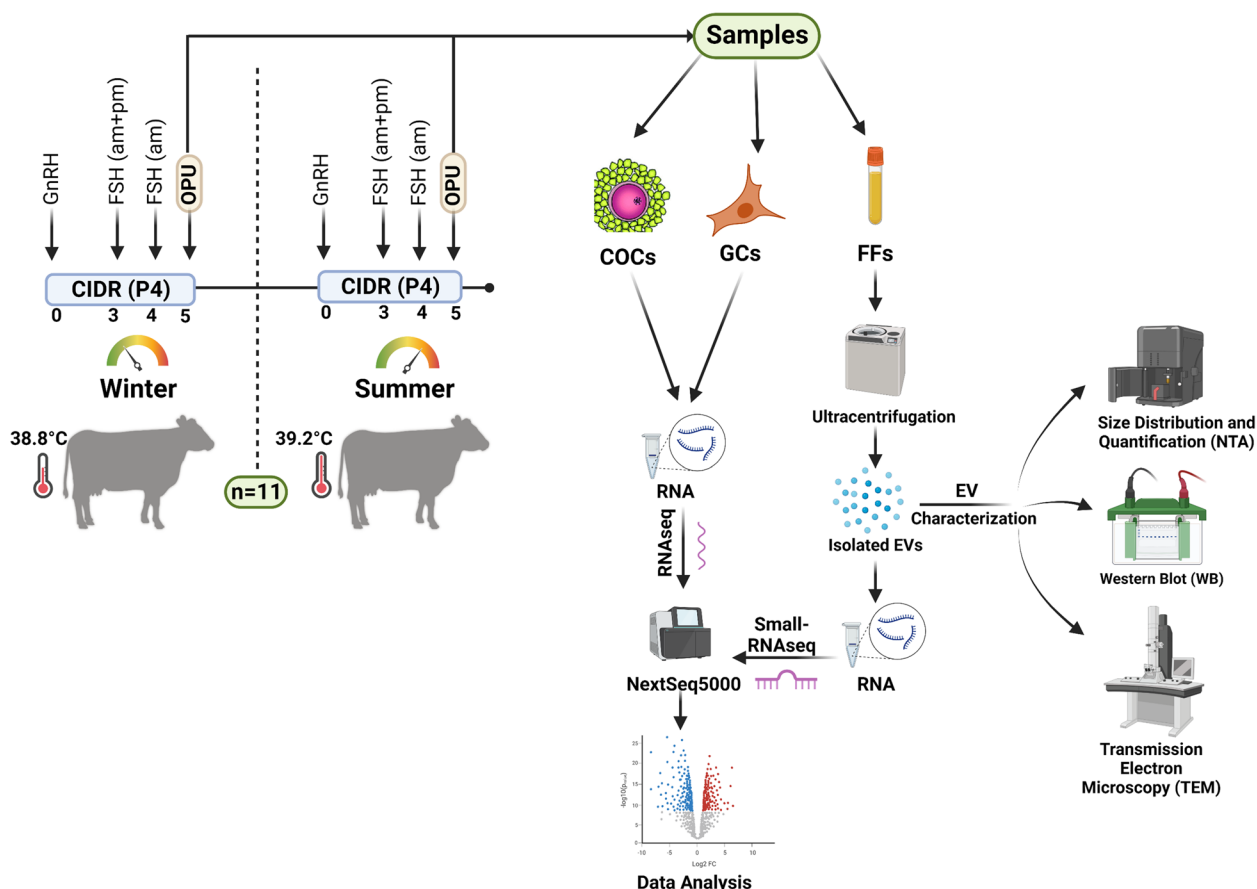


**Fig. 1** Experimental Design. Dry beef cows ( $n = 11$ ) were subjected to synchronization and stimulation for follicular dynamics. Ovum pick-up (OPU) was conducted on all animals in the summer and winter seasons by ultrasound-guided transvaginal follicle aspiration. The follicular fluids (FFs) were collected from each target group (4 biological replicates/group; 8 mL FF/replicate). EVs were then isolated from the FFs using high-speed ultracentrifugation. Isolated EVs were characterized using NanoSight Tracking Analysis, western blot for EV and cellular marker proteins, and transmission electron microscopy. Total RNA was isolated from FF-EVs and small-RNA library preparation and RNAseq (NextSeq500; Illumina) were performed

System Biosciences, USA), Anti-FLOT1 rabbit polyclonal (1:250 System Biosciences, USA), and Anti-CYTc goat polyclonal (1:350 Santa Cruz Biotechnology, Germany) primary antibodies overnight at 4°C. After washing the membranes with 1×TBST, membranes were incubated with appropriate secondary antibodies conjugated with horseradish peroxidase for 1 h at room temperature protected from light. After washing the membranes, protein bands were visualized using an enhanced chemiluminescence substrate (Bio-Rad Laboratories, USA) and images were acquired using Chemi Doc XRS + chemiluminescence imaging system (Bio-Rad Laboratories, USA).

The morphology of the purified EVs were analyzed using a transmission electron microscope (TEM) according to the methods previously reported [20]. Briefly, a drop of 30 µl purified EVs was placed on parafilm. The EVs drops were covered with Formvar/carbon-coated

grids and allowed to stand for 5 min to absorb the EVs. The grids that contained the EVs were washed with drops of ddH<sub>2</sub>O and fixed by placing them on a 30 µL drop of 2% uranyl acetate. The presence of the EVs on the carbon-coated grids was examined under an electron microscope. TEM imaging was done on a FEI/TFS Tecnai T12 Spirit TEM (FEI Company; Hillsboro, OR, USA), operating at 100 kV, with an AMT CCD.

The concentration and size distribution of isolated EVs were determined using the Zetaview Particle Metrix (Particle Metrix, Germany). Briefly, 10 µl of purified EVs was diluted in 990 µl of sterile PBS and assembled into the Zetaview Laser scattering microscope (Particle Metrix, Germany) fitted with an LM14C laser. For each sample, 11 independent video measurements were recorded at 11 independent positions, and video files were analyzed with ZetaView software version 8.05.12.



All experimental parameters related to EV isolation and characterization have been submitted to the EV-TRACK knowledgebase (<https://evtrack.org>) under the EV-TRACK ID EV220402.

#### **Total RNA extraction, library preparation, and sequencing**

Total RNA including miRNAs was isolated from EVs using a Norgen Exosomal RNA Isolation kit (Norgen, Canada), according to the manufacturer's instructions. On-column DNA digestion was performed to remove genomic DNA contaminants. The RNA concentration and size distribution were analyzed using an Agilent RNA 6000 Pico kit in an Agilent 2100 Bioanalyzer (Agilent Technologies, Santa Clara, CA, USA). Small-RNA libraries were prepared for next-generation sequencing (NGS) using a TruSeq Small RNA Library Prep Kit (Illumina) according to the manufacturer's instructions. Library quantity and quality assessments were performed using a Qubit DNA HS Assay Kit in a Qubit 2.0 Fluorometer (Thermo Fisher Scientific) and an Agilent DNA High Sensitivity kit in an Agilent 2100 Bioanalyzer (Agilent Technologies), respectively. The precise concentration of the libraries was calculated using a quantitative PCR. The libraries were pooled in equimolar ratios and then sequenced in a NovaSeq6000 sequencing instrument (Illumina, Inc., San Diego, CA, USA) as single-end reads (50 bases).

#### **Sequencing data analysis**

FASTQ files were generated for each sample using the software bcl2fastq (Illumina Inc., San Diego, CA), and their quality was checked using the FastQC tool version 0.11.9. Data were analyzed using the software CLC Genomics Workbench, version 21. Raw sequence reads were trimmed based on quality score (Q-score > 30), ambiguous nucleotides (maximum two nucleotides allowed), read length ( $\geq 15$  nucleotides), and adapter sequences were also removed. Reads were mapped to the bovine reference genome (ARS-UCD1.2) and annotated against bovine precursor and mature miRNAs listed in the miRBase database (release 22) using the CLC Genomics Workbench RNA-Seq Analysis and Quantify miRNA tools, respectively, applying the default software parameters. Raw expression data were normalized using the trimmed mean of M-values normalization method (TMM normalization) [28] and presented as TMM-adjusted Counts Per Million (CPM). The CLC Genomics Workbench Differential Expression tool was used for the expression analysis comparison of the two groups. MiRNAs with fold change (FC) > 1.5, p-adjusted value (FDR < 0.1 [29]), and average CPM > 10 were considered differentially expressed (DE). The raw FASTQ files and processed CSV files have been deposited in the NCBI's

Gene Expression Omnibus (GEO) with the accession number GSE221198.

#### **qRT-PCR validation**

To validate the miRNA sequencing data, five DE-miRNAs (three from SUM upregulated and two from down-regulated), as representative candidates, were selected for expression validation using qRT-PCR. For this, three independent EV samples from three different animals were used for total RNA including miRNAs isolation as mentioned above, and selected miRNAs were quantified using specific TaqMan miRNA Assays (Applied Biosystems, Foster City, CA, USA) using a real-time PCR (BioRad Inc.) according to the manufacturer's instructions. In brief, for each miRNA, a total of 5 ng RNA was reverse transcribed (RT) using a TaqMan microRNA Reverse Transcription Kit (Thermo Fisher Scientific, Waltham, MA) and miRNA-specific stem-loop primer (Applied Biosystems). RT reaction mixtures were incubated at 16 °C then 42 °C for 30 min each, followed by 85 °C for 5 min. The qRT-PCR was conducted in a 20  $\mu$ l reaction mixture containing 2  $\mu$ l cDNA sample, 1  $\mu$ l FAM-labeled TaqMan assay, 10  $\mu$ l TaqMan Universal PCR Master Mix (Applied Biosystems), and 7  $\mu$ l nuclease-free water. Reaction conditions were as follows: initial denaturation at 95 °C for 10 min, followed by 40 cycles consisting of denaturation at 95 °C for 15 s, annealing, and extension at 60 °C for 60 s. Expression values were normalized to the geometric mean of miR-125 and miR-191 expression levels, the most stably expressed miRNA across all samples based on the NormFinder analysis. Statistical analysis of miRNA expression data was performed using Student's t-test and statistical significance was identified at  $P \leq 0.05$ .

#### **Target gene prediction and ontological classification**

Genes targeted by the DE-miRNA were identified using the human homologous miRNAs in the miRWalk database [30] to enhance the target prediction. Within the miRWalk, validated target genes from miRTarBase (version 7.0) and commonly target genes predicted by TargetScan (version 7.1) and miRDB (release 5.0) were selected for ontological classification analysis using the DAVID bioinformatics web tool (<https://david.abcc.ncifcrf.gov/>). Pathways and biological processes (BP) were determined from the KEGG pathway database [31], and GOTERM\_BP\_DIRECT annotation set, respectively. Terms with low gene count (< 5 genes) were filtered out from the pathways and BP lists. The interaction networks of the targeted genes and the identified pathways were constructed with Cytoscape [32].

### Sequence motif analysis

Sequence-specific miRNA motifs (4–6 base) that are enriched in the up-regulated miRNAs compared to the down-regulated miRNAs (control sequences) were identified using Multiple Expectation Maximization for Motif Elicitation (MEME) suite v. 5.5.0 [33]. Motifs that commonly appeared in at least 50% of the submitted miRNAs were selected for further analysis. To determine the motif-associated RNA binding proteins (RBPs), the selected motifs were submitted to the TOMTOM motif comparison tool [34] using the RNA database.

## Results

### Identification and characterizations of isolated EVs

Follicular fluid-derived EVs from SUM and WIN groups were characterized morphologically and molecularly according to the recommendations set by the International Society of Extracellular Vesicles (ISEV) [35]. The western blot analysis showed that the FF-EVs from both groups are enriched with the transmembrane proteins FLOT1, CD63, and TSG101 protein. Moreover, the mitochondrial protein marker, Cytochrome C was absent in the EV samples, but present in bovine GCs (Fig. 2A), confirming the purity of the EVs and the absence of cellular contaminants in the EV preparation. TEM imaging showed the presence of EVs with visible bilipid membranes within the acceptable size ranges (Fig. 2B). The NTA analysis showed that the concentration of

EV samples from both groups was within the range of  $3.5 \times 10^{11}$  to  $1.75 \times 10^{12}$  particles/mL with no significant differences between the groups. Similarly, the EVs median size was around 114 nm in both groups with no significant differences (Fig. 2C). The total RNA isolated from the EV samples were analyzed for their integrity and the electropherogram analysis showed a clear peak for the small RNA size ranges and the absence of rRNA subunit peaks (18 s and 28 s) which characterize the cellular RNA, indicating no cellular contamination in the isolated EV samples (Fig. 2E).

### MiRNA expression profiles and differential expression analysis

A total of eight small-RNA libraries were constructed with approximately 20 million reads per library that passed the QC parameters with an average of 85% mapped to the bovine reference genome. Out of the mapped reads, an average of 6.6% were annotated to the bovine miRNAs from the miRBase database (Supplementary Table S1). Based on the miRNA expression profiles, principal component analysis (PCA) and heatmap exhibited a clear clustering of the replicates of each group (Fig. 3). A total of 243 and 248 miRNAs were considered as expressed (>10 CPM) in the SUM and WIN groups, respectively, with 232 miRNAs being expressed in common and a total of 11 and 16 miRNAs were found to be exclusively detected in SUM and WIN groups,

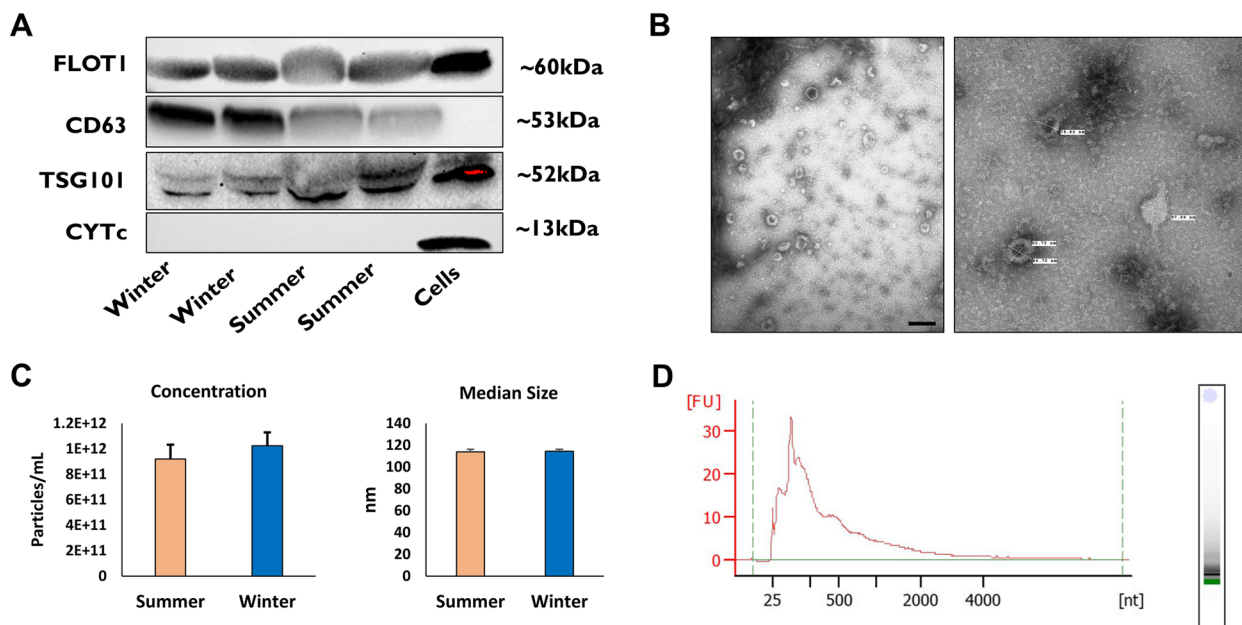


**Fig. 2** Morphological and molecular characterization of EVs. Western blot analysis of EVs marker proteins FLOT1, CD63, and TSG101 and cellular protein contamination indicator CYTc (A). Transmission electron microscope (TEM) imaging shows a clear morphology of EVs with a cross-sectional size of the diameter, scale bar = 200 nm (B). The concentration and median size of the isolated EVs using the NTA analysis (C). The RNA size distribution of EVs shows the presence of the peak of small RNA and the absence of the 18 s and 28 s ribosomal RNA peaks (D)

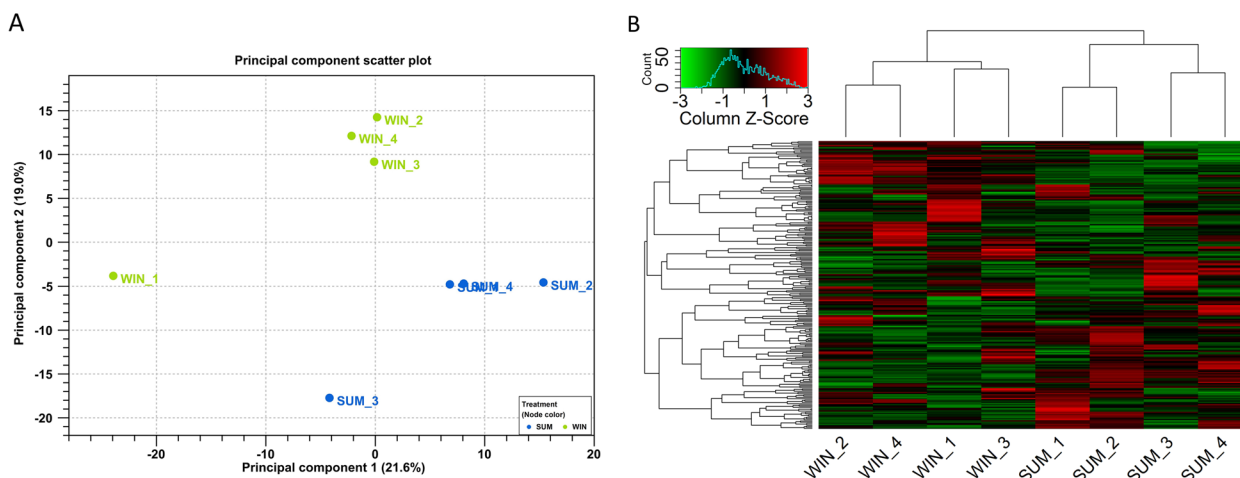


**Fig. 3** Small-RNA sequence data overview. Principal Component Analysis (A). Heatmap and hierarchical clustering of expressed miRNAs. Red and green colors represent high and low expressed miRNAs, respectively (B). SUM: summer group; WIN: winter group

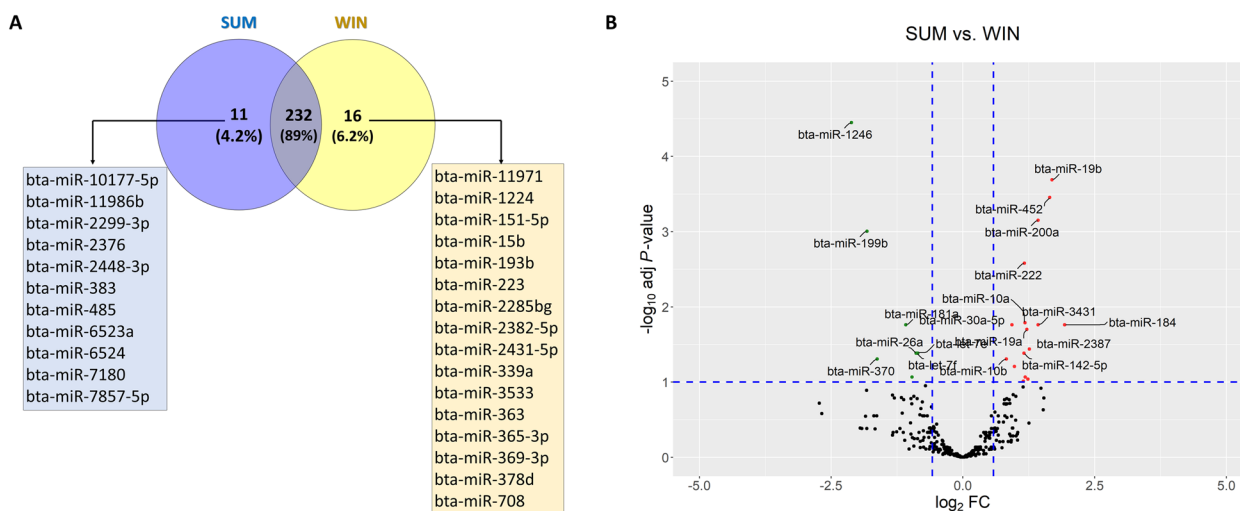


**Fig. 4** Differentially expressed miRNAs. Venn diagram for commonly and exclusively expressed miRNAs in the FF-EVs of summer (SUM) and winter (WIN) groups (A). Volcano plot of expressed miRNAs. Up- and downregulated miRNAs in the SUM compared to the WIN FF-EV groups are labeled with red and green points, respectively (B)

respectively (Fig. 4A). The top 20 highly expressed miRNAs are presented in Table 1 and the complete list of all expressed miRNAs is presented in Supplementary Table S2. Among the top 20 expressed miRNAs, 18 miRNAs were commonly detected in both groups. Interestingly, miR-148a, miR-99a-5p, miR-10b, and miR-143 were the top four miRNAs in both groups and accounting for approximately 52 and 62% of the total miRNA sequence reads in the SUM and WIN groups, respectively (Table 1).

Differential expression analysis indicated a total of 24 miRNAs as significantly differentially expressed between the two groups ( $FC > 1.5$ ,  $FDR < 0.1$ ,  $CPM > 10$ ). A group of 16 miRNAs was up-regulated and 8 miRNAs were down-regulated in the SUM compared to the WIN group (Table 2 and Fig. 4B). MiR-184, miR-19b, and miR-452 were up-regulated and miR-1246, miR-199b, and miR-370 were downregulated with more than three folds in the SUM compared to the WIN group. Interestingly, five

**Table 1** List of top 20 most abundant miRNAs in the extracellular vesicles obtained from follicular fluids from SUM and WIN groups

Name	SUM	Name	WIN
bta-miR-148a	335,249	bta-miR-148a	265,292.7
bta-miR-99a-5p	146,729.6	bta-miR-99a-5p	100,948.9
bta-miR-10b	131,675.5	bta-miR-10b	74,287.82
bta-miR-143	48,985.58	bta-miR-143	46,764.92
bta-let-7b	29,996.77	bta-miR-26a	43,106.6
bta-miR-10a	28,665.65	bta-let-7a-5p	35,540.64
bta-miR-26a	23,293.75	bta-miR-1246	35,452.23
bta-let-7a-5p	21,727.87	bta-let-7b	28,978.75
bta-miR-320a	20,767.93	bta-let-7i	23,237.47
bta-miR-21-5p	15,787.62	bta-miR-320a	22,398.35
bta-let-7i	15,370.83	bta-let-7f	21,824.77
bta-miR-151-3p	13,991.34	bta-let-7c	15,041.31
bta-miR-27b	12,268.99	bta-miR-21-5p	14,597.74
bta-miR-128	11,920.15	bta-miR-10a	12,673.24
bta-let-7f	11,891.01	bta-miR-423-5p	10,828.92
bta-miR-25	11,251.66	bta-miR-151-3p	10,629.91
bta-miR-378	10,807.93	bta-miR-146b	10,133.07
bta-let-7c	10,641.53	bta-miR-128	9588.558
bta-miR-423-5p	10,115.64	bta-let-7 g	9309.91
bta-miR-146b	9761.571	bta-miR-27b	9140.885

The expression values indicated as the mean of TMM-adjusted Counts Per Million (CPM)

DE-miRNAs (miR-10a, miR-10b, miR-26a, let-7f, and miR-1246) were also among the top 20 expressed miRNA lists.

#### qRT-PCR validation

To validate the sequencing data, a group of 5 DE-miRNAs was selected and quantified using qRT-PCR. All miRNAs exhibited the same expression pattern as in the miRNAseq data ( $P < 0.05$ ) except for miR-222, which showed the same pattern but with no statistical significance between the two groups (Fig. 5).

#### Target gene prediction and gene ontology

Target gene analysis revealed a total of 871 and 909 genes as potential targets of up and downregulated miRNAs, in SUM group respectively, with 140 genes commonly targeted by both groups of miRNAs. Ontological classification of these genes showed that EGFR tyrosine kinase inhibitor resistance, ErbB signaling, p53 signaling, and endocrine resistance were the top significant pathways targeted by the upregulated miRNAs in the SUM compared to the WIN group. On the other hand, cellular senescence, JAK-STAT signaling, FoxO signaling, and hippo signaling were the top significant pathways targeted by the downregulated

**Table 2** Differentially expressed (DE) miRNAs in extracellular vesicles obtained from follicular fluids of SUM compared to WIN group

Name	Sequence	FC	FDR
bta-miR-184	TGGACGGAGAAGCTGATAAGGGT	3.81	0.017351
bta-miR-19b	TGTGCAAATCCATGCAAACTGA	3.23	0.000205
bta-miR-452	TGTTGTCAGAGGAACTGAGAC	3.14	0.000351
bta-miR-200a	TAACACTGTCTGGTAACGATGTT	2.69	0.000704
bta-miR-3431	CCTCAGTCAGCCTTGTTGGATGT	2.69	0.017329
bta-miR-2387	TGGAAGGCCTGGCTTTCAGCGG	2.40	0.036309
bta-miR-2408	CACGTGTGTGAGCTCAGCCGG	2.35	0.091029
bta-miR-19a	TGTGCAAATCTATGCAAACTGA	2.32	0.019879
bta-miR-95	TTCAACGGGTATTTATTGAGCA	2.27	0.085596
bta-miR-10a	TACCCTGTAGATCCGAATTTGTG	2.26	0.0162
bta-miR-222	AGCTACATCTGGCTACTGGGT	2.25	0.00262
bta-miR-142-5p	CATAAAGTAGAAAGCACTAC	2.23	0.041243
bta-miR-24-3p	TGGCTCAGTTCAGCAGGAACAG	2.21	0.097153
bta-miR-2483-3p	AAACATCTGTTGGTTGAGAGA	1.97	0.062057
bta-miR-30a-5p	TGTAACATCCTCGACTGGAAGCT	1.91	0.017351
bta-miR-10b	TACCCTGTAGAACCGAATTTGTG	1.77	0.049396
bta-let-7e	TGAGGTAGGAGTTGTATAGT	-1.81	0.041243
bta-let-7f	TGAGGTAGTAGATTGTATAGTT	-1.83	0.041243
bta-miR-26a	TTCAAGTAATCCAGGATAGGCT	-1.85	0.041243
bta-miR-126-3p	CGTACCGTGAGTAATAATGCG	-1.95	0.085596
bta-miR-181a	AACATTCAACGCTGTCGGTGAGTT	-2.12	0.017351
bta-miR-370	GCCTGCTGGGGTGGAACTGGT	-3.09	0.049396
bta-miR-199b	CCCAGTGTTTAGACTATCTGTTC	-3.53	0.000985
bta-miR-1246	AATGGATTTTGGAGCAGG	-4.33	3.54E-05

FC Fold Change, FDR False Discovery Rate

miRNAs (Fig. 6, Supplementary Table S3). Regulation of transcription and gene expression were the top significant biological processes targeted by the elevated miRNAs in the SUM compared to the WIN group while regulation of cell proliferation and cell cycle were the top significant biological processes targeted by the downregulated miRNAs (Fig. 6, Supplementary Table S4). The interaction networks of the top 5 pathways and their corresponding genes targeted by the DE miRNAs are presented in Fig. 7.

#### miRNA sequence motif analysis

To identify potential sequence motifs and the corresponding RNA binding proteins associated with the regulation of the packaging and release of the candidate miRNAs into EVs in response to thermal stress, we performed motif sequence analysis of the miRNAs that were enriched in SUM FF-EVs compared to the miRNAs that were enriched in WIN FF-EVs group. We identified four different motifs (4–5 bases). Two of them significantly appeared on more than 80% (13 out of 16) of the



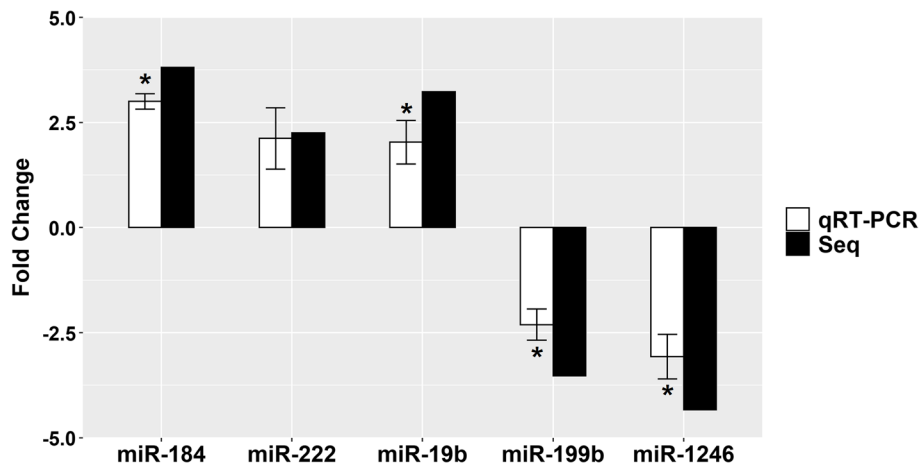


**Fig. 5** qRT-PCR analysis. Expression validation of the selected DE-miRNAs in comparison to the RNAseq (Seq) analysis. \*Statistical significance between the summer and winter FF-EV groups ( $P < 0.05$ )

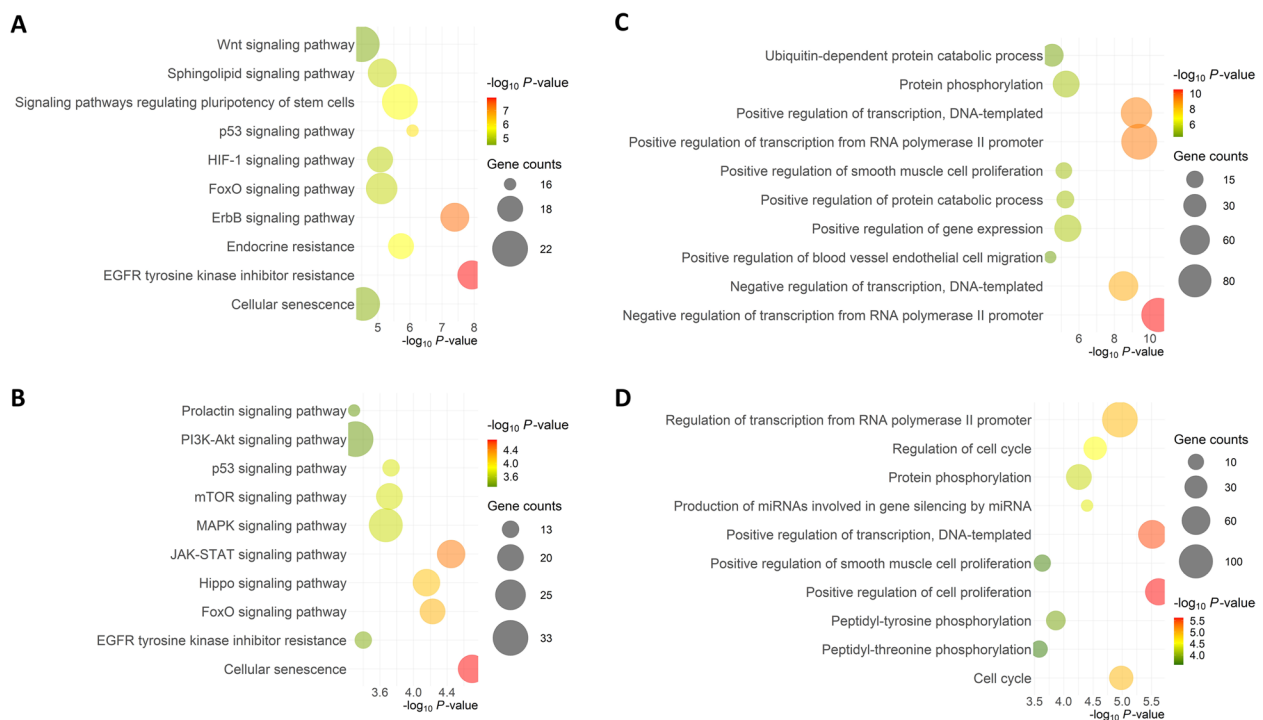
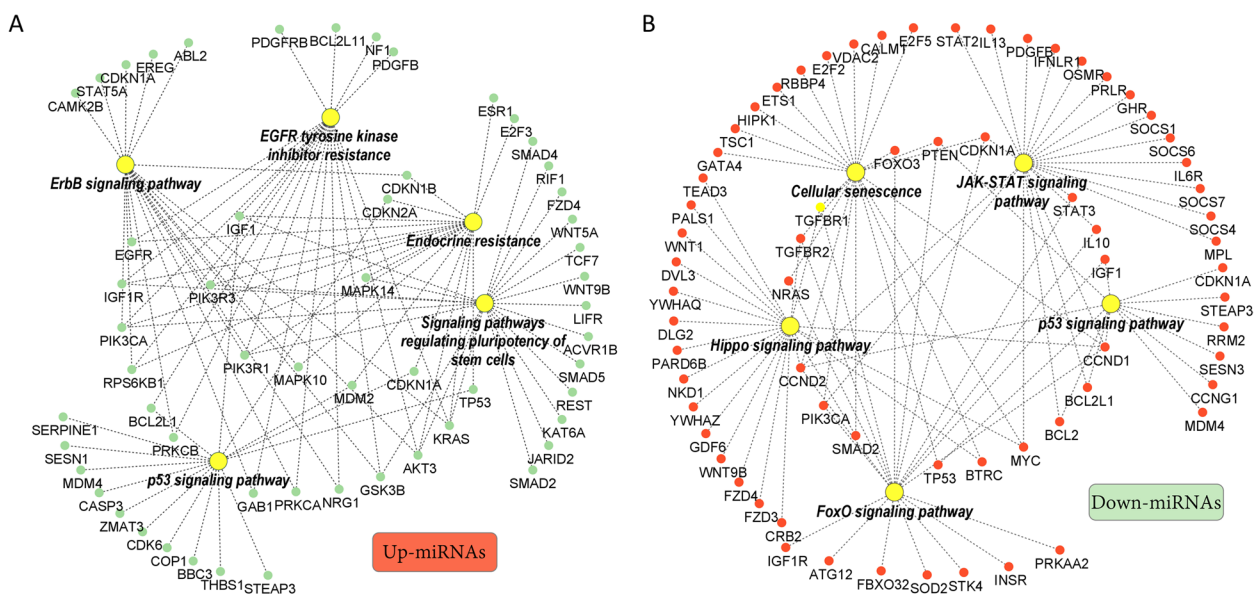


**Fig. 6** Ontological Classification. Top 10 pathways and biological processes targeted by the up- (A and C, respectively) and down-regulated miRNAs (B and D, respectively) in the summer compared to the winter FF-EV groups

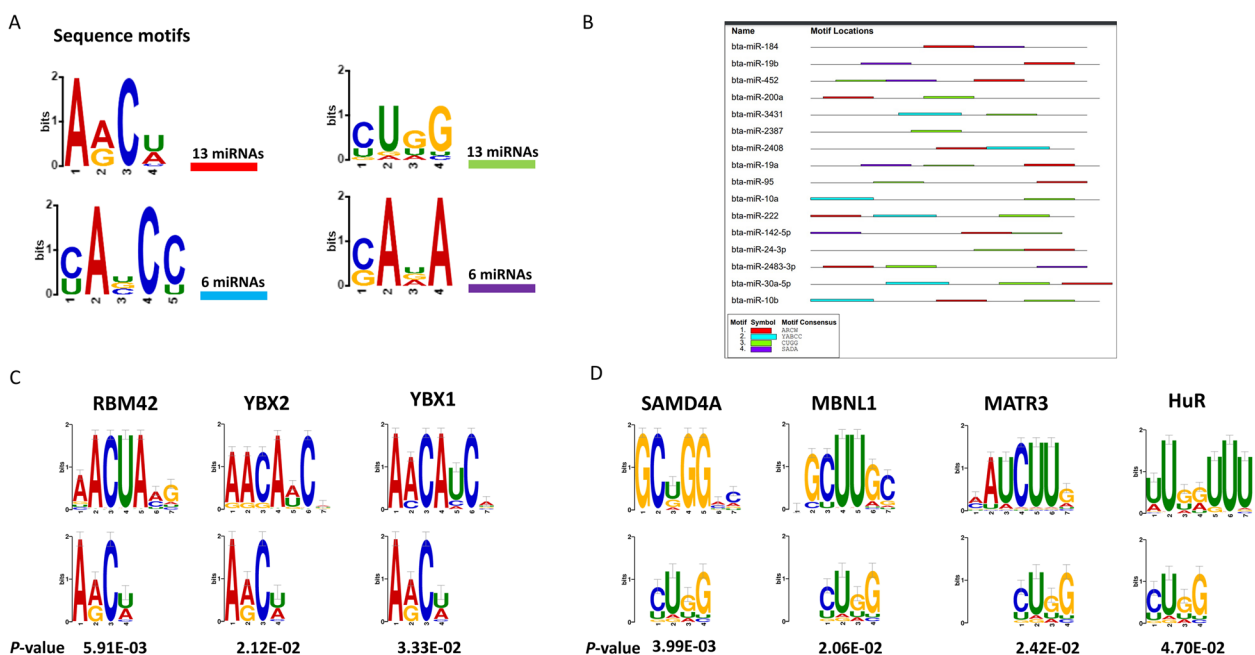
up-regulated miRNAs (Fig. 8A and B; Table 3). RBP-specific motif matching showed that the first motif (AACU) is potentially targeted by RBM42, YBX2, and YBX1 proteins (Fig. 8C) while the second motif (CUGG) is potentially targeted by SAMD4A, MBNL1, MATR3, and HuR proteins (Fig. 8D).

### Discussion

Extracellular vesicles are known to shuttle ample bioactive molecules (mRNA, miRNA, proteins, and lipids) reflecting the physiological status of the secreting cells, [36, 37] leading to alterations in gene expression and function in recipient cells [38]. Our previous studies



**Fig. 7** Interaction networking. The top 5 pathways and their corresponding genes targeted by up (A) or downregulated (B) miRNAs in the summer compared to the winter group

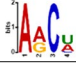
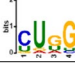


**Fig. 8** miRNA sequence motif analysis. Four identified motifs in different numbers of the up-regulated miRNAs in the summer compared to the winter group (A). The locations and distribution of the identified motifs on the up-regulated miRNAs (B). The alignments of the AACU (C) and CUGG (D) motifs with the known RNA binding protein motifs ( $P < 0.05$ )

indicated that the bovine FF-EVs-miRNA profiles are associated with oocyte developmental competence [39] and the post-calving metabolic status of dairy cows [40]. We have also reported that, under in vitro conditions, bovine granulosa cells subjected to thermal stress release EVs with different miRNA cargo have the potential to

shuttle protective messages to recipient cells inducing thermotolerance against subsequent HS [20]. Therefore, unveiling the ovarian FF-EV cargoes in response to environmental thermal stress conditions in vivo will aid to elucidate the EV-mediated molecular response and potential impact on follicular development and oocyte

**Table 3** The identified motif positions on the up-regulated miRNAs in the SUM compared to the WIN group

miRNA	P-Value		miRNA	P-Value	
bta-miR-19a	3.89E-03	UGUGCAA <u>AUC</u> UAUGCAA <u>AACUG</u> A	bta-miR-30a-5p	3.66E-03	UGUAAACA <u>UCCUCG</u> A <u>CU</u> GGAAAGCU
bta-miR-452	3.89E-03	UGUUUGCAGAGGA <u>AACUG</u> AGAC	bta-miR-2483-3p	3.66E-03	AAACA <u>CU</u> GGUUGGUUGAGAGA
bta-miR-19b	3.89E-03	UGUGCAA <u>UCCAUGCAA</u> AACUGA	bta-miR-222	3.66E-03	AGCUACAUCUGGCUA <u>CU</u> GGGU
bta-miR-184	3.89E-03	UGGACGGAG <u>AACUG</u> AUAAGGGU	bta-miR-2387	3.66E-03	UGGAAGGCC <u>CU</u> GGCUUUGCAGCG
bta-miR-30a-5p	1.18E-02	UGUAAACA <u>UCCUCG</u> A <u>CU</u> GGAAAGCU	bta-miR-200a	3.66E-03	UACACUGU <u>CU</u> GGUAACGAUGUU
bta-miR-2483-3p	1.18E-02	<u>AAACA</u> UCUGGUUGGUUGAGAGA	bta-miR-10b	2.31E-02	UACCCUGUAGAACCGAA <u>UUU</u> GUG
bta-miR-24-3p	1.18E-02	UGGCUCAGUUCAGCAGG <u>AAC</u> AG	bta-miR-10a	2.31E-02	UACCCUGUAGA <u>UCCGAA</u> <u>UUU</u> GUG
bta-miR-222	1.18E-02	<u>AGCU</u> ACAUCUGGCUACUGGGU	bta-miR-452	2.31E-02	UG <u>UUU</u> GCAGAGGAACUGAGAC
bta-miR-2408	1.18E-02	CACGUGUGAG <u>AG</u> CUAGCCGG	bta-miR-24-3p	3.44E-02	UGGCUCAGUUCAG <u>CAGG</u> AACAG
bta-miR-200a	1.18E-02	<u>UAA</u> CACUGUCUGGUAACGAUGUU	bta-miR-95	3.44E-02	UUCAAC <u>GGG</u> UAUUUUUUGAGCA
bta-miR-142-5p	1.58E-02	CAUAAAGUAGAA <u>AGC</u> ACUAC	bta-miR-3431	3.94E-02	CCUCAGUCAGCCUU <u>GUGG</u> AUGU
bta-miR-95	1.58E-02	UUCAACGGGUAAUU <u>UUG</u> AGCA	bta-miR-142-5p	6.89E-02	CAUAAAGUAGAAAGC <u>ACU</u> AC
bta-miR-10b	1.88E-02	UACCCUGUAG <u>AACCG</u> AUUUGUG	bta-miR-19a	8.74E-02	UGUGCAA <u>AUC</u> UAUGCAAACUGA

growth. Here we aimed to investigate the changes in FF-EV-coupled miRNAs in beef cows when comparing winter and summer seasons. The deviation in EV-miRNA profiles in summer compared to the winter season may in part explain the abnormal ovarian function, follicular development, and infertility-associated problems due to climate change-induced thermal stress in dairy and beef animals [41, 42].

Among the top 20 highly abundant miRNAs, 18 were commonly expressed in both groups including miR-148a and miR-99a, the top highly expressed miRNAs in the FF-EVs with no significant differences between the groups. Similarly, miR-148 was reported as the top expressed miRNA in FF-EVs from large and small follicles in goats [43]. In human FFs, miR-99a was specifically enriched in the FF-EVs and considered as a regulator of the ovarian follicle developmental process to include meiosis resumption [44]. In another study, the expression of miR-148a and miR-99a in FF-EVs was highly correlated with IVF outcomes, specifically day-3 embryo quality [45]. The detection of these candidate miRNAs at a higher level in both seasons indicates their potential housekeeping role in ovarian function. In the same top 20 miRNAs list, miR-10a and miR-10b were expressed amid both groups and were significantly upregulated in the SUM compared to the WIN group. Both miRNAs belong to the conserved mir-10 family and are known to play key roles in inducing apoptosis and repressing cell proliferation in ovarian GCs through suppressing the brain-derived neurotrophic factor (BDNF) and TGF-β pathways [46]. Additionally, miR-10a has been reported to promote human GC tumor development by targeting PTEN-AKT/Wnt pathways [47] and regulating lipid metabolism and steroid hormone synthesis in sheep GCs [48]. Previously, it has been validated that miR-10a directly recognizes and targets the *BCL6* transcript and negatively regulates its expression leading to cellular apoptosis [49]. In correlation with

HS, miR-10a was suggested to be involved in the stress response pathway regulation via its repression of a number of p53/Rb networks' key genes [50]. Therefore, our results indicate the negative impact of seasonal HS on ovarian function is mediated by the enrichment of miR-10a and miR-10b in EVs released in response to thermal stress. Another interesting miRNA from the same top 20 miRNAs list was miR-26a which exhibited a significant downregulation in the SUM compared to the WIN group. A similar study in heat-stressed Holstein cows showed that the expression of miR-26a was downregulated in serum and found to be involved in stress and immune response-related processes [51]. Moreover, a HS-induced increase in corticosterone hormone is similarly found to be associated with the reduction in miR-26a in rat serum EVs [52]. In addition, it has been confirmed that miR-26a targets *Exh2* and plays a critical role in regulating apoptosis in mouse ovarian GCs [53].

In the current study, we found a total of 24 DE-miRNAs in the FF-EVs between the SUM and WIN groups. Among the upregulated miRNAs, four (miR-19a, miR-19b, miR-30a-5p, and miR-200a) were commonly identified as highly expressed in the serum of heat-stressed Holstein cows [51]. In another study, miR-19a and miR-19b were identified among the circulatory miRNAs that were highly expressed in lactating Holstein cows under summer HS conditions and were correlated with functions governing responses to stress and oxidative damage [54]. Moreover, heat shock during in vitro maturation of bovine oocytes was shown to increase the expression of miR-19b in embryos, indicating a carryover impact of HS on miRNAs in the cellular response [55]. In humans, miR-19b has been reported as an inhibitor of GC proliferation by directly targeting *IGF-1* and the reduction in its expression could reverse the results [56] suggesting the important regulatory and specific role of miR-19b in GCs and could explain the oocyte quality and fertility

reduction during the summer season. The top-upregulated miRNA in the SUM group was miR-184. This miRNA is associated with an inhibitory effect on GC estradiol production [57] and was found to be increased in bovine GCs at day 7 compared to day 3 of the estrous cycle [58].

On the other hand, a cluster of eight miRNAs was downregulated in the SUM FF-EVs compared to the WIN group including miR-181a and miR-1246. Both miRNAs showed a clear reduction in buffalo GCs cultured under thermal stress conditions [59] and are known to be involved in stress and immune responses [51, 60]. Inhibition of miR-181a expression suppresses apoptosis and ROS production in human chondrocyte cells [61] and reduces heat stress damage through the upregulation of antioxidant-related genes and the downregulation of apoptotic genes in bovine peripheral blood mononuclear cells [62]. Contrary to our findings, miR-1246 was found to be highly enriched in the serum of dairy cows under environmental HS [51, 54], as well as, in the GC-released EVs under in vitro elevated culture temperature [20]. However, the expression of miR-1246 in correlation with HS seems to be time-dependent, as in cattle and buffalo fibroblast cells, the expression of miR-1246 declined immediately after HS and then increased gradually during the recovery period post-HS [60]. This discrepancy in the differential expression results of EV-miRNA-1246 might be associated with the timing of exposure and recovery to thermal stress. Taken together, our data revealed that seasonal HS can induce the enrichment of FF-EV-coupled miRNAs, with a potential negative impact on ovarian function (i.e. miR-10 family) and the depletion of candidate miRNAs (i.e. miR-26a) with the potential beneficial role in ovarian physiology.

Although EV miRNA abundance is altered under suboptimal physiological conditions to include HS, little is known about the mechanism associated with their sorting into EVs versus their cellular retention. Recently, the regulatory role of RBPs in the packaging of particular RNA molecules into EVs following the recognition and binding of specific sequence motifs is emerging among different models [63, 64]. Sequence motif analysis for EV-coupled miRNAs enriched in SUM samples revealed two specific motifs appearing on 13 out of the 16 upregulated miRNAs and recognized by specific RBPs. One of those motifs was found to be potentially recognized and bound by Y-box binding proteins (YBX1 and YBX2). These proteins are members of a large family of proteins with the cold shock domain that play roles in several cellular processes including proliferation and stress

response [65, 66]. A study by Guarino et al. reported that oxidative stress enhances the secretion of YBX1 protein from stressed cells which significantly inhibits proliferation and leads to cell cycle arrest in receiving cells [67]. Y-box proteins have been identified as the main components in the formation of ribonucleoprotein particles with the different types of RNA including mRNA and miRNA [68] and play a role in sorting these RNA molecules into EVs [69]. Regarding miRNAs, it has been evidenced that YBX1 binds to and is required for the sorting of specific miRNAs into EVs released from the HEK293T human cell line [70]. Another interesting RBP that matched with the same sequence motif was RBM42, which together with the hnRNP K is part of the stress granules. Under stress conditions, both proteins co-localize and interact to form cytoplasmic foci in order to maintain cellular ATP levels [71]. The expression of these proteins in correlation to stress conditions, as well as, their matching of common sequence motifs among the upregulated miRNAs in the SUM group could explain a potential mechanism involved in sorting and releasing of these FF-EV-miRNAs under HS conditions. However, further studies are required to specifically investigate the role of miRNA motifs and RBPs in regulating the sorting and packaging of stress associated miRNAs into EVs and the role that this interplay drives on follicular cells stress response and survival under various environmental and physiological suboptimal conditions.

## Conclusions

Overall, the current study revealed that FF-EV-miRNA profiles can be explored to investigate the follicular level response of cows to seasonal changes and this might partially explain altered ovarian physiology, follicular development, and infertility-associated issues resulting from climate change-induced seasonal thermal stress in the dairy and beef industry. Based on the differentially expressed miRNAs, we suggest that the negative impact of HS on ovarian function is mediated by abnormal alterations in EV-coupled molecular signaling within the follicular microenvironment, as shown by the contrasting finding when comparing summer and winter EV-miRNAs. However, further studies are needed to confirm and investigate the exact role of these EV-miRNAs concerning seasonal effects and fertility. The current study also identified potential targets of future therapeutic and managerial intervention to tackle the negative impact of environmental thermal stress in cattle with potential translation to seasonal human infertility problems.



## Supplementary Information

The online version contains supplementary material available at <https://doi.org/10.1186/s13048-023-01181-7>.

**Additional file 1: Table S1.** Summary of sequence reads mapped to the bovine reference genome and annotated against bovine miRNAs listed in the mirBase database. **Table S2.** A complete list of all expressed miRNAs indicated as the mean of TMM-adjusted Counts Per Million (CPM) value. **Table S3.** KEGG pathway analysis for genes targeted by the differentially expressed miRNAs in SUM vs. WIN group. **Table S4.** Biological process (BP) analysis for genes targeted by the differentially expressed miRNAs in SUM vs. WIN group.

### Acknowledgements

The authors acknowledge the University of Colorado, Boulder EM Services Core Facility in the MCDB Department as well as D.N. Rao Veeramachaneni and Jennifer S. Palmer at Colorado State University, for their assistance with TEM imaging. Nano-particle tracking analysis was performed by Ms. Mindy A. Meyers from the Department of Clinical Sciences at Colorado State University. The authors thank Jhon Fredy Rodriguez and Edna Ballesteros from Breeding Tech LLC (Madisonville – Texas) for their technical assistance during the OPU procedures.

### Authors' contributions

Conceptualization: D.T., A.G.D., Experimental work: A.G., K.J., N.G.M., D.H., C.S.R., Data analysis: A.G., N.G.M., Interpretation of data: A.G., D.T., A.G.D., Writing of original draft: A.G., Manuscript editing: D.T., A.G.D., N.G.M., Supervision: D.T., A.G.D., Funding acquisition: D.T., A.G.D., All authors have read and agreed to the published version of this manuscript.

### Availability of data and materials

The raw FASTQ files and processed CSV files of the miRNA sequencing data have been deposited in the NCBI's Gene Expression Omnibus (GEO) repository with the accession number GSE221198. All parameters related to EV experiments are available on the EV-TRACK knowledgebase (EV-TRACK ID: EV220402).

### Declarations

#### Ethics approval and consent to participate

All procedures involving cows were approved by the Animal Care and Use Committee of the University of Florida with the approval number IACUC202200000706.

#### Competing interests

There is no conflict of interest to declare.

#### Author details

<sup>1</sup>Department of Biomedical Sciences, Animal Reproduction and Biotechnology Laboratory (ARBL), Department of Biomedical Sciences, Colorado State University, Fort Collins, CO, USA. <sup>2</sup>Department of Animal Production, Faculty of Agriculture, Cairo University, Giza 12613, Egypt. <sup>3</sup>North Florida Research and Education Center, Institute of Food and Agricultural Sciences, University of Florida, Marianna, FL, USA.

Received: 19 January 2023 Accepted: 5 May 2023

Published online: 23 May 2023

### References

- Thornton P, Nelson G, Mayberry D, Herrero M. Impacts of heat stress on global cattle production during the 21st century: a modelling study. *Lancet Planet Heal*. 2022;6:e192–201. Available from: <http://www.thelancet.com/article/S254251962200002X/fulltext>. [cited 2022 Dec 15].
- Rojas-Downing MM, Nejadhashemi AP, Harrigan T, Woznicki SA. Climate change and livestock: Impacts, adaptation, and mitigation. *Clim Risk Manag*. 2017;16:145–63. Available from: <https://linkinghub.elsevier.com/retrieve/pii/S221209631730027X>. [cited 2022 Dec 15].
- Khan A, Dou J, Wang Y, Jiang X, Khan MZ, Luo H, et al. Evaluation of heat stress effects on cellular and transcriptional adaptation of bovine granulosa cells. *J Anim Sci Biotechnol*. 2020;11:25. Available from: <https://jasbs.ci.biomedcentral.com/articles/10.1186/s40104-019-0408-8>.
- Roth Z. Effect of Heat Stress on Reproduction in Dairy Cows: Insights into the Cellular and Molecular Responses of the Oocyte. *Annu Rev Anim Biosci*. 2017;5:151–70. Available from: <https://pubmed.ncbi.nlm.nih.gov/27732786/>. [cited 2022 Nov 11].
- Friedman E, Voet H, Reznikov D, Wolfenson D, Roth Z. Hormonal treatment before and after artificial insemination differentially improves fertility in subpopulations of dairy cows during the summer and autumn. *J Dairy Sci*. 2014;97:7465–75. Available from: <https://pubmed.ncbi.nlm.nih.gov/25306276/>. [cited 2022 Nov 14].
- Renis F De, Scaramuzzi RJ. Heat stress and seasonal effects on reproduction in the dairy cow—a review. *Theriogenology*. 2003;60:1139–51. Available from: <https://linkinghub.elsevier.com/retrieve/pii/S0093691X03001262>. [cited 2023 Mar 3].
- Herbut P, Angrecka S, Walczak J. Environmental parameters to assessing of heat stress in dairy cattle—a review. *Int J Biometeorol*. 2018;62:2089–97. Available from: <https://link.springer.com/article/10.1007/s00484-018-1629-9>. [cited 2023 Mar 3].
- Rocha A, Randel RD, Broussard JR, Lim JM, Blair RM, Roussel JD, et al. High environmental temperature and humidity decrease oocyte quality in *Bos taurus* but not in *Bos indicus* cows. *Theriogenology*. 1998;49:657–65. Available from: <https://pubmed.ncbi.nlm.nih.gov/10732044/>. [cited 2022 Nov 14].
- Al-Katanani YM, Paula-Lopes FF, Hansen PJ. Effect of Season and Exposure to Heat Stress on Oocyte Competence in Holstein Cows. *J Dairy Sci*. 2002;85:390–6. Available from: <https://pubmed.ncbi.nlm.nih.gov/11913699/>. [cited 2022 Nov 14].
- Roth Z. Heat stress, the follicle, and its enclosed oocyte: mechanisms and potential strategies to improve fertility in dairy cows. *Reprod Domest Anim*. 2008;43 Suppl 2:238–44. Available from: <http://doi.wiley.com/10.1111/j.1439-0531.2008.01168.x>. [cited 2018 Jan 10].
- Shehab-El-Deen MAMM, Fadel MS, van Soom A, Saleh SY, Maes D, Leroy JLMR. Circadian rhythm of metabolic changes associated with summer heat stress in high-producing dairy cattle. *Trop Anim Health Prod*. 2010;42:1119–25. Available from: <https://pubmed.ncbi.nlm.nih.gov/20221690/>. [cited 2022 Nov 14].
- Shan Q, Ma F, Wei J, Li H, Ma H, Sun P. Physiological Functions of Heat Shock Proteins. *Curr Protein Pept Sci*. 2020;21:751–60. Available from: <https://pubmed.ncbi.nlm.nih.gov/31713482/>. [cited 2022 Dec 12].
- Saeed-Zidane M, Linden L, Salilew-Wondim D, Held E, Neuhoef C, Tholen E, et al. Cellular and exosome mediated molecular defense mechanism in bovine granulosa cells exposed to oxidative stress. *PLoS One*. 2017;12:e0187569. <https://journals.plos.org/plosone/article?id=10.1371/journal.pone.0187569>. [cited 2022 Dec 12].
- Tsutsumi S, Neckers L. Extracellular heat shock protein 90: A role for a molecular chaperone in cell motility and cancer metastasis. *Cancer Sci*. 2007;98:1536–9. Available from: <https://onlinelibrary.wiley.com/doi/full/10.1111/j.1349-7006.2007.00561.x>. [cited 2022 Dec 12].
- Hightower LE, Guidon PT. Selective release from cultured mammalian cells of heat-shock (stress) proteins that resemble gliosis transfer proteins. *J Cell Physiol*. 1989;138:257–66. Available from: <https://onlinelibrary.wiley.com/doi/full/10.1002/jcp.1041380206>. [cited 2022 Dec 12].
- Gilchrist R, Ritter L, Armstrong D. Oocyte–somatic cell interactions during follicle development in mammals. *Anim Reprod Sci*. 2004;82–83:431–46. Available from: <https://pubmed.ncbi.nlm.nih.gov/15271471/>. [cited 2022 Nov 17].
- György B, Szabó TG, Pásztói M, Pál Z, Misják P, Aradi B, et al. Membrane vesicles, current state-of-the-art: emerging role of extracellular vesicles. *Cell Mol Life Sci*. 2011;68:2667–88. Available from: <https://link.springer.com/article/10.1007/s00018-011-0689-3>. [cited 2022 Nov 17].
- Taylor DD, Gercel-Taylor C. The origin, function, and diagnostic potential of RNA within extracellular vesicles present in human biological fluids. *Front Genet*. 2013;4. Available from: <https://pubmed.ncbi.nlm.nih.gov/23908664/>. [cited 2022 Dec 9].

19. Yáñez-Mó M, Siljander PR-M, Andreu Z, Zavec AB, Borràs FE, Buzas EI, et al. Biological properties of extracellular vesicles and their physiological functions. *J Extracell Vesicles*. 2015;4:27066. Available from: <http://www.ncbi.nlm.nih.gov/pubmed/25979354>. [cited 2020 Apr 6].
20. Gebremedhn S, Gad A, Aglan HS, Laurincik J, Prochazka R, Salilew-Wondim D, et al. Extracellular vesicles shuttle protective messages against heat stress in bovine granulosa cells. *Sci Rep*. 2020;10:1–19. <https://doi.org/10.1038/s41598-020-72706-z>. [cited 2020 Sep 25].
21. Nehammer C, Podolska A, Mackowiak SD, Kagiás K, Pocock R. Specific microRNAs Regulate Heat Stress Responses in *Caenorhabditis elegans*. *Sci Rep*. 2015;5:8866. Available from: <https://www.nature.com/articles/srep08866>. [cited 2022 Dec 12].
22. Li Q, Yang C, Du J, Zhang B, He Y, Hu Q, et al. Characterization of miRNA profiles in the mammary tissue of dairy cattle in response to heat stress. *BMC Genomics*. 2018;19:1–11. Available from: <https://bmcbgenomics.biomedcentral.com/articles/10.1186/s12864-018-5298-1>. [cited 2022 Dec 12].
23. Leung AKL, Sharp PA. MicroRNA Functions in Stress Responses. *Mol Cell*. 2010;40:205–15. Available from: <https://linkinghub.elsevier.com/retrieve/pii/S1097276510007550>.
24. Leung AKL, Sharp PA. Molecular Cell Review MicroRNA Functions in Stress Responses. 2010. Available from: <http://www.mirbase.org/>. [cited 2022 Dec 12].
25. Sarlo Davila KM, Hamblen H, Hansen PJ, Dikmen S, Oltenacu PA, Mateescu RG. Genetic parameters for hair characteristics and core body temperature in a multibreed Brahman–Angus herd1. *J Anim Sci*. 2019;97:3246–52. [cited 2023 Jan 13]. Available from: <https://academic.oup.com/jas/article/97/8/3246/5520432>.
26. Mateescu RG, Sarlo-Davila KM, Dikmen S, Rodriguez E, Oltenacu PA. The effect of Brahman genes on body temperature plasticity of heifers on pasture under heat stress. *J Anim Sci*. 2020;98:1–9. Available from: <https://academic.oup.com/jas/article/98/5/skaa126/5823257>. [cited 2023 Jan 13].
27. St-Pierre NR, Cobanov B, Schnitkey G. Economic Losses from Heat Stress by US Livestock Industries. *J Dairy Sci*. 2003;86:E52–77. Available from: <https://linkinghub.elsevier.com/retrieve/pii/S0022030203740405>. [cited 2023 Jan 13].
28. Robinson MD, Oshlack A. A scaling normalization method for differential expression analysis of RNA-seq data. *Genome Biol*. 2010;11:R25. Available from: <http://genomebiology.biomedcentral.com/articles/10.1186/gb-2010-11-3-r25>. [cited 2018 Oct 2].
29. Benjamini Y, Hochberg Y. Controlling the false discovery rate: a practical and powerful approach to multiple testing. *J R Stat Soc Ser B*. 1995;57:289–300. <https://doi.org/10.1111/j.2517-6161.1995.tb02031.x>. [cited 2019 Feb 25].
30. Sticht C, De La Torre C, Parveen A, Gretz N. miRWalk: An online resource for prediction of microRNA binding sites. *PLoS One*. 2018;13:e0206239. <https://doi.org/10.1371/journal.pone.0206239>. [cited 2021 Aug 24].
31. Ogata H, Goto S, Sato K, Fujibuchi W, Bono H, Kanehisa M. KEGG: Kyoto Encyclopedia of Genes and Genomes. *Nucleic Acids Res*. 1999;27:29–34. Available from: <http://www.ncbi.nlm.nih.gov/pubmed/9847135>. [cited 2018 Oct 4].
32. Shannon P. Cytoscape: A Software Environment for Integrated Models of Biomolecular Interaction Networks. *Genome Res*. 2003;13:2498–504. Available from: <http://www.genome.org/cgi/doi/10.1101/gr.1239303>. [cited 2018 Oct 4].
33. Bailey TL, Johnson J, Grant CE, Noble WS. The MEME Suite. *Nucleic Acids Res*. 2015;43:W39–49. Available from: <https://pubmed.ncbi.nlm.nih.gov/25953851/>. [cited 2022 Oct 18].
34. Gupta S, Stamatoyannopoulos JA, Bailey TL, Noble WS. Quantifying similarity between motifs. *Genome Biol*. 2007;8. Available from: <https://pubmed.ncbi.nlm.nih.gov/17324271/>. [cited 2022 Oct 18].
35. Théry C, Witwer KW, Aikawa E, Alcaraz MJ, Anderson JD, Andriantsitohaina R, et al. Minimal information for studies of extracellular vesicles 2018 (MISEV2018): a position statement of the International Society for Extracellular Vesicles and update of the MISEV2014 guidelines. *J Extracell Vesicles*. 2018;7:1535750. Available from: <https://www.tandfonline.com/doi/abs/10.1080/20013078.2018.1535750>. [cited 2021 Oct 11].
36. Valadi H, Ekström K, Bossios A, Sjöstrand M, Lee JJ, Lötvall JO. Exosome-mediated transfer of mRNAs and microRNAs is a novel mechanism of genetic exchange between cells. *Nat Cell Biol*. 2007;9:654–9. Available from: <http://www.nature.com/articles/ncb1596>. [cited 2020 Mar 22].
37. Godakumara K, Dissanayake K, Hasan MM, Kodithuwakku SP, Fazeli A. Role of extracellular vesicles in intercellular communication during reproduction. *Reprod Domest Anim*. 2022;57:14–21. Available from: <https://pubmed.ncbi.nlm.nih.gov/35837748/>. [cited 2022 Nov 30].
38. Thomou T, Mori MA, Dreyfuss JM, Konishi M, Sakaguchi M, Wolfrum C, et al. Adipose-derived circulating miRNAs regulate gene expression in other tissues. *Nature*. 2017;542:450–5. Available from: <https://www.nature.com/articles/nature21365>. [cited 2022 Dec 1].
39. Sohel MMH, Hoelker M, Noferesti SS, Salilew-Wondim D, Tholen E, Looft C, et al. Exosomal and Non-Exosomal Transport of Extra-Cellular microRNAs in Follicular Fluid: Implications for Bovine Oocyte Developmental Competence. *PLoS One*. 2013;8:e78505. Available from: <https://journals.plos.org/plosone/article?id=10.1371/journal.pone.0078505>. [cited 2022 Nov 30].
40. Hailay T, Hoelker M, Poirier M, Gebremedhn S, Rings F, Saeed-Zidane M, et al. Extracellular vesicle-coupled miRNA profiles in follicular fluid of cows with divergent post-calving metabolic status. *Sci Rep*. 2019;9:12851. Available from: <http://www.nature.com/articles/s41598-019-49029-9>. [cited 2020 Apr 15].
41. Miretti S, Lecchi C, Cecilian F, Baratta M. MicroRNAs as Biomarkers for Animal Health and Welfare in Livestock. *Front Vet Sci*. 2020;7:985.
42. Reza AMMT, Choi Y-J, Han SG, Song H, Park C, Hong K, et al. Roles of microRNAs in mammalian reproduction: from the commitment of germ cells to peri-implantation embryogenesis. *Biol Rev*. 2019;94:415–38. Available from: <https://onlinelibrary.wiley.com/doi/10.1111/brv.12459>. [cited 2023 Mar 30].
43. Ding Q, Jin M, Kalds P, Meng C, Wang H, Zhong J, et al. Comparison of MicroRNA Profiles in Extracellular Vesicles from Small and Large Goat Follicular Fluid. *Animals*. 2021;11:3190. Available from: <https://pubmed.ncbi.nlm.nih.gov/34827922/>. [cited 2022 Aug 12].
44. Santonocito M, Vento M, Guglielmino MR, Battaglia R, Wahlgren J, Ragusa M, et al. Molecular characterization of exosomes and their microRNA cargo in human follicular fluid: bioinformatic analysis reveals that exosomal microRNAs control pathways involved in follicular maturation. *Fertil Steril*. 2014;102:1751–1761.e1. Available from: <https://linkinghub.elsevier.com/retrieve/pii/S0015028214020640>. [cited 2020 Apr 20].
45. Martinez RM, Liang L, Racowsky C, Dioni L, Mansur A, Adir M, et al. Extracellular microRNAs profile in human follicular fluid and IVF outcomes. *Sci Rep*. 2018;8:17036. Available from: <http://www.nature.com/articles/s41598-018-35379-3>. [cited 2020 Feb 13].
46. Jijie T, Yanzhou Y, Hoi-Hung AC, Zi-Jiang C, Wai-Yee C. Conserved miR-10 family represses proliferation and induces apoptosis in ovarian granulosa cells. *Sci Rep*. 2017;7:41304. Available from: <https://www.nature.com/articles/srep41304>. [cited 2022 Nov 28].
47. Tu J, Cheung H-H, Lu G, Chen Z, Chan W-Y. MicroRNA-10a promotes granulosa cells tumor development via PTEN-AKT/Wnt regulatory axis. *Cell Death Dis*. 2018;9:1076. Available from: <https://www.nature.com/articles/s41419-018-1117-5>. [cited 2023 Mar 2].
48. Dai T, Kang X, Yang C, Mei S, Wei S, Guo X, et al. Integrative Analysis of miRNA-mRNA in Ovarian Granulosa Cells Treated with Kisspeptin in Tan Sheep. *Animals*. 2022;12:2989. Available from: <https://www.mdpi.com/2076-2615/12/21/2989>.
49. Fan Q, Meng X, Liang H, Zhang H, Liu X, Li L, et al. miR-10a inhibits cell proliferation and promotes cell apoptosis by targeting BCL6 in diffuse large B-cell lymphoma. *Protein Cell*. 2016;7:899–912. Available from: <https://link.springer.com/article/10.1007/s13238-016-0316-z>. [cited 2022 Nov 28].
50. Ovcharenko D, Stölzel F, Poitz D, Fierro F, Schaich M, Neubauer A, et al. miR-10a overexpression is associated with NPM1 mutations and MDM4 downregulation in intermediate-risk acute myeloid leukemia. *Exp Hematol*. 2011;39. Available from: <https://pubmed.ncbi.nlm.nih.gov/21784052/>. [cited 2022 Nov 28].
51. Zheng Y, Chen K, Zheng X, Li H, Wang G. Identification and bioinformatics analysis of microRNAs associated with stress and immune response in serum of heat-stressed and normal Holstein cows. *Cell Stress Chaperones*. 2014;19:973–81. [cited 2020 Sep 23]. Available from: <http://link.springer.com/10.1007/s12192-014-0521-8>.
52. Lafourcade CA, Fernández A, Ramírez JP, Corvalán K, Carrasco MÁ, Iturriaga A, et al. A role for mir-26a in stress: a potential sEV Biomarker and

- modulator of excitatory neurotransmission. *Cells*. 2020;9. [cited 2022 Nov 30]. Available from: <https://www.mdpi.com/2073-4409/9/6/1364>.
53. Huo S, Qi H, Si Y, Li C, Du W. MicroRNA 26a targets Ezh2 to regulate apoptosis in mouse ovarian granulosa cells. *Syst Biol Reprod Med*. 2021;67:221–9. <https://doi.org/10.1080/19396368.2021.1895362>.
  54. Lee J, Lee S, Son J, Lim H, Kim E, Kim D, et al. Analysis of circulating-micro-RNA expression in lactating Holstein cows under summer heat stress. *PLoS One*. 2020;15:e0231125. <https://doi.org/10.1371/journal.pone.0231125>. [cited 2020 Sep 23].
  55. Souza V das GP de, Souza GT de, Lemos DR de, Guimaraes JM de O, Quintão CCR, Munk M, et al. Heat shock during in vitro maturation of bovine oocytes disturbs bta-miR-19b and DROSHA transcripts abundance after in vitro fertilization. *Reprod Domest Anim*. 2021;56:1128–36. Available from: <https://onlinelibrary.wiley.com/doi/full/10.1111/rda.13956>. [cited 2022 Dec 6].
  56. Zhong Z, Li F, Li Y, Qin S, Wen C, Fu Y, et al. Inhibition of microRNA-19b promotes ovarian granulosa cell proliferation by targeting IGF-1 in polycystic ovary syndrome. *Mol Med Rep*. 2018;17:4889. Available from: [pmc/articles/PMC5865948/](https://pubmed.ncbi.nlm.nih.gov/33809236/). [cited 2023 Mar 2].
  57. Sirotkin A V, Ovcharenko D, Grossmann R, Lauková M, Mlynček M. Identification of MicroRNAs controlling human ovarian cell steroidogenesis via a genome-scale screen. *J Cell Physiol*. 2009;219:415–20. Available from: <https://onlinelibrary.wiley.com/doi/full/10.1002/jcp.21689>. [cited 2023 Mar 2].
  58. Salilew-Wondim D, Ahmad I, Gebremedhn S, Sahadevan S, Hossain MM, Rings F, et al. The Expression Pattern of microRNAs in Granulosa Cells of Subordinate and Dominant Follicles during the Early Luteal Phase of the Bovine Estrous Cycle. *PLoS One*. 2014;9:e106795. Available from: <https://journals.plos.org/plosone/article?id=10.1371/journal.pone.0106795>. [cited 2023 Mar 2].
  59. Faheem MS, Ghanem N, Gad A, Procházka R, Dessouki SM. Adaptive and Biological Responses of Buffalo Granulosa Cells Exposed to Heat Stress under In Vitro Condition. *Animals*. 2021;11:794. Available from: <https://pubmed.ncbi.nlm.nih.gov/33809236/>. [cited 2022 Dec 6].
  60. Shandilya UK, Sharma A, Sodhi M, Mukesh M. Heat stress modulates differential response in skin fibroblast cells of native cattle (*Bos indicus*) and riverine buffaloes (*Bubalus bubalis*). *Biosci Rep*. 2020;40. [cited 2020 Sep 22]. Available from: <https://portlandpress.com/bioscirep/article/40/2/BSR20191544/221965/Heat-stress-modulates-differential-response-in>.
  61. Cheleschi S, Tenti S, Mondanelli N, Corallo C, Barbarino M, Giannotti S, et al. MicroRNA-34a and MicroRNA-181a Mediate Visfatin-Induced Apoptosis and Oxidative Stress via NF- $\kappa$ B Pathway in Human Osteoarthritis Chondrocytes. *Cells*. 2019;8:874. [cited 2022 Dec 6]. Available from: <https://pubmed.ncbi.nlm.nih.gov/31405216/>.
  62. Chen K-L, Fu Y-Y, Shi M-Y, Li H-X. Down-regulation of miR-181a can reduce heat stress damage in PBMCs of Holstein cows. *Vitr Cell Dev Biol - Anim*. 2016;52:864–71. Available from: <https://pubmed.ncbi.nlm.nih.gov/27130682/>. [cited 2020 Sep 23].
  63. Fabbiano F, Corsi J, Gurrieri E, Trevisan C, Notarangelo M, D'Agostino VG. RNA packaging into extracellular vesicles: An orchestra of RNA-binding proteins? *J Extracell Vesicles*. 2020;10. Available from: <https://pubmed.ncbi.nlm.nih.gov/33391635/>. [cited 2022 Feb 22].
  64. Garcia-Martin R, Wang G, Brandão BB, Zanotto TM, Shah S, Kumar Patel S, et al. MicroRNA sequence codes for small extracellular vesicle release and cellular retention. *Nature*. 2022;601:446–51. Available from: <https://www.nature.com/articles/s41586-021-04234-3>. [cited 2022 Feb 17].
  65. Mordovkina D, Lyabin DN, Smolin EA, Sogorina EM, Ovchinnikov LP, Eliseeva I. Y-Box Binding Proteins in mRNP Assembly, Translation, and Stability Control. *Biomolecules*. 2020;10:591. Available from: <https://www.mdpi.com/2218-273X/10/4/591/htm>. [cited 2022 Dec 1].
  66. Eliseeva IA, Kim ER, Guryanov SG, Ovchinnikov LP, Lyabin DN. Y-box-binding protein 1 (YB-1) and its functions. *Biochem*. 2011;76:1402–33. Available from: <https://pubmed.ncbi.nlm.nih.gov/22339596/>. [cited 2022 Dec 1].
  67. Guarino AM, Troiano A, Pizzo E, Bosso A, Vivo M, Pinto G, et al. Oxidative Stress Causes Enhanced Secretion of YB-1 Protein that Restrains Proliferation of Receiving Cells. *Genes (Basel)*. 2018;9:513. Available from: <https://pubmed.ncbi.nlm.nih.gov/30360431/>. [cited 2022 Dec 1].
  68. Mordovkina D, Lyabin DN, Smolin EA, Sogorina EM, Ovchinnikov LP, Eliseeva I. Y-Box Binding Proteins in mRNP Assembly, Translation, and Stability Control. *Biomolecules*. 2020;10:591. Available from: [pmc/articles/PMC7226217/](https://pubmed.ncbi.nlm.nih.gov/33391635/). [cited 2022 Dec 5].
  69. Yanshina DD, Kossinova OA, Gopanenko A V, Krasheninina OA, Malygin AA, Venyaminova AG, et al. Structural features of the interaction of the 3'-untranslated region of mRNA containing exosomal RNA-specific motifs with YB-1, a potential mediator of mRNA sorting. *Biochimie*. 2018;144:134–43. Available from: <https://pubmed.ncbi.nlm.nih.gov/29133115/>. [cited 2022 Dec 5].
  70. Shurtleff MJ, Temoche-Diaz MM, Karfilis K V, Ri S, Schekman R. Y-box protein 1 is required to sort microRNAs into exosomes in cells and in a cell-free reaction. *Elife*. 2016;5. Available from: <https://elifesciences.org/articles/19276>. [cited 2022 Dec 1].
  71. Fukuda T, Naiki T, Saito M, Irie K. hnRNP K interacts with RNA binding motif protein 42 and functions in the maintenance of cellular ATP level during stress conditions. *Genes to Cells*. 2009;14:113–28. Available from: <https://pubmed.ncbi.nlm.nih.gov/19170760/>. [cited 2022 Dec 1].

## Publisher's Note

Springer Nature remains neutral with regard to jurisdictional claims in published maps and institutional affiliations.

### Ready to submit your research? Choose BMC and benefit from:

- fast, convenient online submission
- thorough peer review by experienced researchers in your field
- rapid publication on acceptance
- support for research data, including large and complex data types
- gold Open Access which fosters wider collaboration and increased citations
- maximum visibility for your research: over 100M website views per year

At BMC, research is always in progress.

Learn more [biomedcentral.com/submissions](https://biomedcentral.com/submissions)

